MCB
Journals.ASM.org

# Regulation of Chaperone Effects on a Yeast Prion by Cochaperone Sgt2

**Denis A. Kiktev, Jesse C. Patterson,* Susanne Müller,* Bhawana Bariar,* Tao Pan,* and Yury O. Chernoff**

School of Biology and Parker H. Petit Institute for Bioengineering & Bioscience, Georgia Institute of Technology, Atlanta, Georgia, USA

**Yeast prions, based on self-seeded highly ordered fibrous aggregates (amyloids), serve as a model for human amyloid diseases. Propagation of yeast prions depends on the balance between chaperones of the Hsp100 and Hsp70 families. The yeast prion [*PSI*$^+$] can be eliminated by an excess of the chaperone Hsp104. This effect is reversed by an excess of the chaperone Hsp70-Ssa. Here we show that the actions of Hsp104 and Ssa on [*PSI*$^+$] are modulated by the small glutamine-rich tetratricopeptide cochaperone Sgt2. Sgt2 is conserved from yeast to humans, has previously been implicated in the guided entry of tail-anchored proteins (GET) trafficking pathway, and is known to interact with Hsps, cytosolic Get proteins, and tail-anchored proteins. We demonstrate that Sgt2 increases the ability of excess Ssa to counteract [*PSI*$^+$] curing by excess Hsp104. Deletion of *SGT2* also restores trafficking of a tail-anchored protein in cells with a disrupted GET pathway. One region of Sgt2 interacts both with the prion domain of Sup35 and with tail-anchored proteins. Sgt2 levels are increased in response to the presence of a prion when major Hsps are not induced. Our data implicate Sgt2 as an amyloid "sensor" and a regulator of chaperone targeting to different types of aggregation-prone proteins.**

Ordered cross-β fibrous protein aggregates (amyloids) are associated with a variety of human diseases, including fatal and incurable Alzheimer's and Huntington's diseases (reviewed in references 19 and 34). Amyloids spread by nucleated polymerization via immobilizing a soluble protein of the same sequence and converting it into an amyloid form. Prion diseases (such as Creutzfeldt-Jakob disease in humans, scrapie in sheep, and bovine spongiform encephalopathy [BSE], or "mad cow disease," in cattle) are caused by infectious amyloids, termed prions (15, 47). A number of endogenous prion proteins have been identified in the yeast *Saccharomyces cerevisiae* (reviewed in references 35 and 39). Most yeast prions are intracellular amyloids inherited in a non-Mendelian fashion (via cytoplasm) and containing QN-rich prion domains that resemble mammalian proteins associated with polyglutamine disorders such as Huntington's disease. Some yeast prions are pathogenic to the yeast "host" (41, 68), thus establishing yeast as a model for studying the pathogenic amyloids. Other yeast prions are widespread in nature, pointing to potentially positive biological effects (23). By transmitting phenotypic changes not associated with DNA variations, prions provide an additional mechanism of inheritance, which may play an important role in both pathology and evolution. Understanding the cellular control of prion propagation and clearance in yeast sheds light on mechanisms that control the spread of mammalian and human amyloids and may lead to the development of antiamyloid therapies.

[*PSI*$^+$], one of the most extensively studied yeast prions, is a self-perpetuating polymer of the translation termination factor Sup35, or eRF3 (reviewed in reference 35). [*PSI*$^+$]-carrying cells are defective in translation termination, thus providing a convenient phenotypic assay for [*PSI*$^+$] based on the readthrough of stop codons (nonsense suppression). Much of our knowledge about the propagation of yeast prions, including the establishment of a crucial role of the chaperone machinery in prion propagation, initially came from experiments on the [*PSI*$^+$] model that were later extended to other prions. [*PSI*$^+$] propagation requires an intermediate level of the chaperone Hsp104 (12), as inactivation or overproduction of Hsp104 cures yeast cells of [*PSI*$^+$] (see Fig. 1A). Most other known yeast amyloid-based prions also require Hsp104 but are not cured by Hsp104 overproduction (reviewed in references 35, 51, and 53). Hsp104 is known to promote disaggregation of heat-damaged proteins after stress (22), and existing evidence (35) supports a model (32) postulating that the requirement of Hsp104 for prion propagation is due to its ability to fragment prion polymers, thus generating "seeds" for new rounds of polymerization. It was also proposed that [*PSI*$^+$] curing by Hsp104 overproduction occurs due to monomerization of polymers in the presence of high levels of Hsp104 (32). However, direct evidence for this mechanism is lacking, and other mechanisms, such as impairment of prion segregation in cell divisions at high Hsp104 levels, have also been discussed (35, 44).

Conserved chaperones of the Hsp70 and Hsp40 families cooperate with Hsp104 in both solubilization of stress-damaged proteins and prion propagation (reviewed in references 35, 51, and 54). Notably, members of the different yeast Hsp70 subfamilies exhibit different effects on [*PSI*$^+$] curing by excess Hsp104. Hsp70-Ssb (represented by two proteins, Ssb1 and -2) promotes [*PSI*$^+$] curing by excess Hsp104 (3, 13), while excess Hsp70-Ssa (represented by Ssa1, -2, -3, and -4) counteracts [*PSI*$^+$] curing by excess Hsp104 (3, 45). Some other genetic alterations, such as

Received 27 June 2012 Returned for modification 7 August 2012
Accepted 28 September 2012
Published ahead of print 8 October 2012

Address correspondence to Yury O. Chernoff, yury.chernoff@biology.gatech.edu.

* Present address: Jesse C. Patterson, Departments of Biology and Biological Engineering, Massachusetts Institute of Technology, Cambridge, Massachusetts, USA; Susanne Müller, Carver College of Medicine, University of Iowa, Iowa City, Iowa, USA; Bhawana Bariar, Department of Biology, University of North Carolina, Charlotte, North Carolina, USA; Tao Pan, Medigen Biotechnology Corp., Taipei City, Taiwan.

Supplemental material for this article may be found at http://mcb.asm.org/.



doi:10.1128/MCB.00875-12

elimination of the ubiquitin-conjugating enzyme Ubc4 (2) or one of the Hsp70/90 cochaperones, Sti1 or Cpr7 (43, 52), as well as the chemical inhibition of Hsp90 (52), also antagonize [*PSI*$^+$] curing by excess Hsp104; however, the mechanisms of these effects remain unknown.

In addition to prions, a variety of other protein aggregates are detected in the yeast cytoplasm. One group of aggregation-prone proteins is represented by tail-anchored (TA) proteins (reviewed in references 8 and 49). These proteins are inserted into membranes (e.g., the endoplasmic reticulum [ER] membrane) via hydrophobic tails, which must be protected from aggregation until proteins reach their target destination. The guided entry of tail-anchored proteins (GET) pathway is responsible for trafficking of TA proteins (57, 65). This pathway includes cytoplasmic Get3, -4, and -5 proteins and transmembrane Get1 and -2 proteins. Failure of the GET pathway, due to genetic alteration of one of its components or under certain physiological conditions, results in the aggregation of TA proteins and remaining cytoplasmic Get proteins (26, 57, 60). Relationships between Get-TA aggregates and other aggregated proteins are poorly understood. Heat shock proteins (Hsps) are known to interact with TA proteins, and these interactions are mediated by the tetratricopeptide cochaperone Sgt2, which also binds Get5 (36, 65).

In this study, we attempted to identify the genetic factors that control elimination of the [*PSI*$^+$] prion by excess Hsp104. We found that alterations of the GET pathway antagonize [*PSI*$^+$] curing caused by excess Hsp104. This effect is associated with the simultaneous induction of the chaperone Hsp70-Ssa and the cochaperone Sgt2 by *get* alterations. Notably, Sgt2 also helps excess Ssa to efficiently reverse the effect of excess Hsp104 on [*PSI*$^+$] in Get$^+$ strains. Our data show that Sgt2 physically interacts with Sup35 and that Sgt2 levels are increased in response to the presence of a prion. These results implicate Sgt2 as a protein that coordinates chaperone interactions with various types of aggregates.

## MATERIALS AND METHODS

**Yeast strains.** *Saccharomyces cerevisiae* strains constructed in this work (see Table S1 in the supplemental material) originated from strain 74-D694, with the genotype *MAT***a** *ade1-14* (UGA) *his3 leu2 trp1 ura3* (12), or from the isogenic haploid strains of the GT81 series, with the genotype *ade1-14* (UGA) *his3 leu2 lys2 trp1 ura3* (11). The original strains typically carried both [*PSI*$^+$] and [*PIN*$^+$] prions. Usually, a "strong" variant of the [*PSI*$^+$] prion, characterized by more translational readthrough and high mitotic stability (35), was used. A weak variant of [*PSI*$^+$] was used for [*PSI*$^+$] destabilization by mild heat shock (44). The [*psi*$^-$ *PIN*$^+$] and [*psi*$^-$ *pin*$^-$] derivatives were obtained after transient overproduction of Hsp104 and after growth on medium with 5 mM guanidine hydrochloride, respectively (14). Construction of the *MAT***a** GT81-derived strains GT146 (*ssb1*Δ *ssb2*Δ) and GT349 (*ubc4*Δ) was described previously (2, 13). Complete gene deletions were constructed by a one-step replacement with cassettes bearing the *HIS5* gene of *Schizosaccharomyces pombe* (an ortholog of *S. cerevisiae HIS3*), a Kan$^r$ gene that determines resistance to G418 in yeast (38), or an *hph* gene that confers resistance to hygromycin B (25). The same procedure was used for tagging chromosomal copies of genes with hemagglutinin (HA) or green fluorescent protein (GFP) (38). Combinations of two or several deletions, as well as combinations of deletions with the tagged constructs, were combined together either via subsequent transplacement steps or through genetic crosses between the otherwise isogenic haploid strains of the GT81 series, followed by sporulation and dissection. Strain pJ69-4A (*MAT***a** *trp1-901 leu2-3,112 ura3-52 his3-200 gal4*Δ *gal80*Δ *GAL2-ADE2 LYS2*::$P_{GAL1}$*-HIS3 met2*::*GAL7-lacZ*) (24) and its *hsp104*Δ derivative were used for two-hybrid assays.

**Plasmids.** Plasmids pYS-GAL104 (11) and pGAL-SSA1 (56), bearing the *HSP104* and *SSA1* genes, respectively, under the control of the galactose-inducible *GAL1,10* promoter ($P_{GAL}$), and the multicopy plasmid pLH101 (45), bearing *SSA1* under the control of its own promoter, were described previously. Multicopy plasmid pFL44-SSB1, bearing *SSB1* under the control of its own promoter, was created by cloning the BamHI/SacI fragment of YCp-SSB1 (46) into pFL44 (7) cut with the same enzymes. Low-copy-number (centromeric) plasmids based on pRS315 (62) and bearing the *SIS1* (33) or *YDJ1* (20) gene under the control of the gene's own promoter were generously provided by D. Cyr. The centromeric plasmid pLH105 (13) contains the *HSP104* gene under the control of a constitutively expressed *GPD* promoter. Plasmid pRS315-GAL104 was constructed by cloning the $P_{GAL}$*-HSP104* sequence from pYS-GAL104 into the BamHI site of pRS315. Plasmids carrying genes that code for proteins with fluorescent tags were generously provided by M. Schuldiner in the case of Get3 (57) and R. Parker in the case of Dcp2 (16), Edc3, and Pub1 (9). Plasmid pRS316-DCP2 was constructed by ligating the DCP-GFP-encoding XbaI fragment from pRP1175 (16) into pRS316 (62) cut by the same enzyme. The 103QP-GFP- and 103QP-RFP-encoding plasmids were described earlier (42). The *GET3* and *SGT2* genes were PCR amplified from genomic DNA of the S288C strain and then cloned into pRS316GAL (37), with the GFP coding sequence from plasmid pmCUP-sGFP (59) added to the 3′ ends of both genes, followed by recloning of the $P_{GAL}$*-GET3-GFP-* or $P_{GAL}$*-SGT2-GFP*-containing fragment into pRS315. Plasmid pRS315-$P_{GAL}$-Sup35NM-dsRed is plasmid pRS315 containing the $P_{GAL}$-carrying XhoI/BamHI fragment from plasmid pRS316-GAL (37) followed by the BamHI/SacII fragment from the plasmid pmCUPNMsGFP (59), coding for the NM domains of Sup35, and by the dsRed2-encoding SacII/HpaI fragment from plasmid pDsRed2-N1 (Clontech). Gene fusions for the two-hybrid analysis of protein interactions involving Sgt2 or its fragments were created by inserting the respective PCR-amplified DNA fragments into the plasmid pACT2 (a gift of S. Elledge [17]), in frame with the N-terminally attached activation domain of Gal4, or pG4BD-0, in frame with the C-terminally attached DNA-binding domain of Gal4 (a gift of R. Brazas). A list of oligonucleotide primers used in this study can be found in Table S2 in the supplemental material. Plasmid pACT2-SUP35N, which codes for the prion domain of Sup35 fused to the C-terminally attached activation domain of Gal4, was described earlier (6). The fusions of Sup35N to the DNA-binding domain of Gal4 were difficult to use due to a residual transcription activation capability. A yeast genomic library based on plasmid p366 was a gift from P. Hieter (21).

**Growth conditions and phenotypic assays.** Standard yeast media and protocols were employed (61). Rich organic medium was yeast extract-peptone-dextrose (YPD) medium. Synthetic dropout media are designated by the supplements that were missing (e.g., "−Ade medium" indicates synthetic medium lacking adenine). The $P_{GAL}$ promoter was induced on solid medium containing 2% galactose instead of glucose or in liquid synthetic medium containing 2% galactose and 2% raffinose instead of glucose. The addition of raffinose to liquid medium was necessary because the strains used in this study grow poorly in liquid medium with galactose but no raffinose. The stringencies for chaperone effects measured in the liquid medium were different from those observed in the plate assay, possibly due to (at least in part) different parameters of $P_{GAL}$ induction in the presence and absence of raffinose. However, differences between the compared strain-plasmid combinations were always in the same direction both in liquid medium and on plates. Yeast cultures were normally incubated at 30°C, unless stated otherwise. The presence of [*PSI*$^+$] was detected by white or light pink growth on YPD and growth on −Ade medium due to readthrough of the *ade1-14* (UGA) reporter; in contrast, the [*psi*$^-$] strains were red on YPD and did not grow on −Ade medium. Temperature sensitivity was tested on rich YPD medium at 37°C. For heat shock experiments, cultures were grown to mid-exponen-

tial phase at 25°C. A mild heat shock for [*PSI*$^+$] curing was performed at 39°C, while a severe heat shock for viability assays was performed at 50°C. Induced thermotolerance was measured after incubating cultures, originally grown at 25°C, at 37°C for 30 min before shifting them to 50°C. Antibiotic sensitivities were detected on YPD medium supplemented with paromomycin (600 μg/ml) or hygromycin (40 μg/ml). Yeast cultures bearing the plasmid pYS-GAL104 were mutagenized in a phosphate-buffered saline (PBS) (pH 7.0) solution containing 3% (GT81 series) or 4% (74-D694) ethyl ester of methanesulfonic acid (EMS) for 1 to 2 h at a concentration of $10^7$ cells/ml, followed by the addition of sodium thiosulfate to a final concentration of 5% (for inactivation of EMS) and spreading of cells on synthetic −Ura medium with galactose in order to maintain the plasmid and to induce $P_{GAL}$-*HSP104* expression. Grown colonies were replica plated onto YPD and −Ade/glucose media for [*PSI*$^+$] detection. To assess [*PSI*$^+$] curing by excess Hsp104 in the plate assay, cultures were replica plated either from synthetic plasmid-selective medium onto −Ade and YPD media (in the case of the plasmid carrying *HSP104* under the control of the constitutive promoter) or from galactose medium onto −Ade/glucose medium selective for the plasmid and onto YPD medium (in the case of the plasmid carrying *HSP104* under the control of the $P_{GAL}$ promoter). For quantitation of [*PSI*$^+$] curing, yeast cultures bearing galactose-inducible constructs were grown in liquid synthetic medium with galactose and raffinose. After specified periods, aliquots were plated onto synthetic glucose-containing medium selective for the respective plasmid(s). The presence of [*PSI*$^+$] in the resulting colonies was detected after replica plating onto YPD and −Ade media.

**Protein analysis.** For protein isolation, cultures were grown in 50 ml of appropriate medium to an optical density at 600 nm ($OD_{600}$) of between 0.5 and 0.7, precipitated by centrifugation, transferred to 1.5-ml centrifuge tubes, washed twice with water, and resuspended in 200 μl of lysis buffer (50 mM Tris-Cl, pH 7.5, 200 mM NaCl, 1% Triton X-100, 0.1% SDS, 1× Complete Mini protease inhibitor cocktail [Roche], 3 mM phenylmethylsulfonyl fluoride, 1 mM *N*-ethylmaleimide). Cells were disrupted by agitation with an equal volume of glass beads for a total of 5 min, with periodic cooling of the mixture on ice. Cell debris was spun down at 4,000 × *g* for 2 min, and the supernatant was used for electrophoresis and Western analysis as described below.

For fractionation of protein aggregates by semidenaturing detergent agarose gel electrophoresis (SDD-AGE) (31), yeast extracts were mixed with a 1/4 volume of 4× loading buffer (240 mM Tris-Cl, pH 6.8, 8% SDS, 40% glycerol, 12% 2-mercaptoethanol, and 0.002% bromophenol blue), loaded onto a 1.8% Tris-acetate-EDTA (TAE)-based agarose gel, and run in 1× TAE buffer with 0.1% SDS. Proteins were then transferred to a nitrocellulose Protran membrane (Whatman) via capillary blotting. The membrane was blocked in 5% dry milk and incubated with the appropriate antibody.

For denaturing polyacrylamide gel electrophoresis (SDS-PAGE) and Western analysis, protein samples in loading buffer (the same as that described above) were boiled in a water bath for 10 min, separated in a 10% SDS-polyacrylamide gel with a 4% stacking gel in Tris-glycine-SDS running buffer (25 mM Tris, 192 mM glycine, 0.1% SDS, pH 8.3), electrotransferred to a Hybond-ECL nitrocellulose membrane (Amersham), blocked in 5% dry milk, and incubated with the appropriate antibody.

For coimmunoprecipitation (co-IP), protein lysates were incubated overnight with anti-HA antibody, followed by a 2-h incubation with protein A agarose beads (Calbiochem). Beads were washed three times with PBS buffer (137 mM NaCl, 2.7 mM KCl, 4.3 mM $Na_2HPO_4$, 1.47 mM $KH_2PO_4$, pH 7.0) to remove unbound proteins. Proteins bound to beads were eluted by adding 1× loading buffer with SDS (60 mM Tris-Cl, pH 6.8, 2% SDS, 10% glycerol, 3% 2-mercaptoethanol, and 0.0005% bromophenol blue).

**Antibodies.** Antibodies to the C-terminal part of Sup35, Hsp104, Hsp70s (Ssa and Ssb), Hsp40s (Ydj1 and Sis1), and Rpl3 (64) were kindly provided by D. Bedwell, S. Lindquist, E. Craig, D. Cyr, and J. Warner, respectively. The antibody to Ade2 was described previously (3). A monoclonal antibody to HA was purchased from Covance.

**Fluorescence microscopy.** Fluorescence microscopy was performed using an Olympus BX41 microscope with an Olympus DP-71 camera. Green and red fluorescence was detected by Endow GFP/EGFP band-pass and Cy3/TRITC (rhodamine)/DiI filter sets, respectively, from Chroma Technology Corporation. All images were taken using a ×100 objective. Cells for fluorescence microscopy were precipitated from exponential-phase cultures by centrifugation, washed twice with water, resuspended in water to a final concentration of approximately $2 \times 10^8$ cells/ml, and placed onto a glass slide (10 μl per sample) under a coverslip for microscopy examination.

## RESULTS

***get* deficiencies impair [*PSI*$^+$] curing by excess Hsp104.** In order to identify mutations that antagonize [*PSI*$^+$] curing by excess Hsp104, we performed EMS mutagenesis followed by a genetic screen (Fig. 1B). A total of 5,700 colonies, originating from the mutagenized cells of two "strong" [*PSI*$^+$] strains of the 74-D694 and GT81 series, were tested. A total of 13 recessive mutants were uncovered after excluding mutations in the *HSP104* plasmid, nonsense suppressors that mimicked effects of [*PSI*$^+$], and other false-positive mutations. Two of these mutations, not allelic to each other and generated in the 74-D694 background, also caused a defect in growth at high temperature (37°C), referred to here as temperature sensitivity (*ts*). Plasmids with two overlapping genomic DNA inserts, able to compensate for both the *ts* phenotype and the [*PSI*$^+$] curing defect in one of these mutants, were isolated from a yeast genomic library. (Identification of another mutant will be described elsewhere.) A deletion analysis of the overlapping portion of the inserts identified *GET2*, encoding one of the major membrane-associated components of the GET trafficking pathway, as a gene responsible for compensation of both phenotypes. Sequencing of the *get2* allele from the mutant strain has shown that it contains a G-to-A transition at nucleotide position 473, converting a codon for tryptophan (TGG) at amino acid position 157 into a stop codon (TAG). This generates a shortened version of the Get2 protein which lacks most of the C-proximal region bearing the transmembrane domains (Fig. 1B). A deletion of the *GET2* gene, as well as a deletion of any other *GET* gene, also impaired [*PSI*$^+$] curing by excess Hsp104 (Fig. 1C). Notably, the elimination of either of the crucial membrane-associated components of the pathway (Get1 or Get2) inhibited [*PSI*$^+$] curing more severely than the elimination of any cytosolic component (Get3, -4, or -5), as seen after prolonged Hsp104 induction (Fig. 1D). This agrees with the appearance of some other phenotypes, such as the previously described (and confirmed by us [see Fig. S1A in the supplemental material]) sensitivity to high temperature and the translational antibiotic hygromycin B, as well as a newly detected sensitivity to paromomycin (see Fig. S1A), in *get1*Δ and *get2*Δ strains but not *get4*Δ and *get5*Δ strains. However, the *get3*Δ strain resembled *get1*Δ and *get2*Δ strains rather than *get4*Δ and *get5*Δ strains in these phenotypes. Pairwise combinations of *get* deletions revealed epistatic interactions, with stronger effects on [*PSI*$^+$] curing prevailing over weaker effects (data not shown).

**Effects of *get2* deletion or mutation on [*PSI*$^+$] are not due to a decrease in Hsp104 levels or activity.** One potential explanation for the effect of *get* alterations on [*PSI*$^+$] curing is a decrease in the Hsp104 level or activity in *get*-deficient strains. However, levels of overexpressed Hsp104 remained unchanged in the *get2*Δ strain compared to the wild type (Fig. 1E). Moreover, background

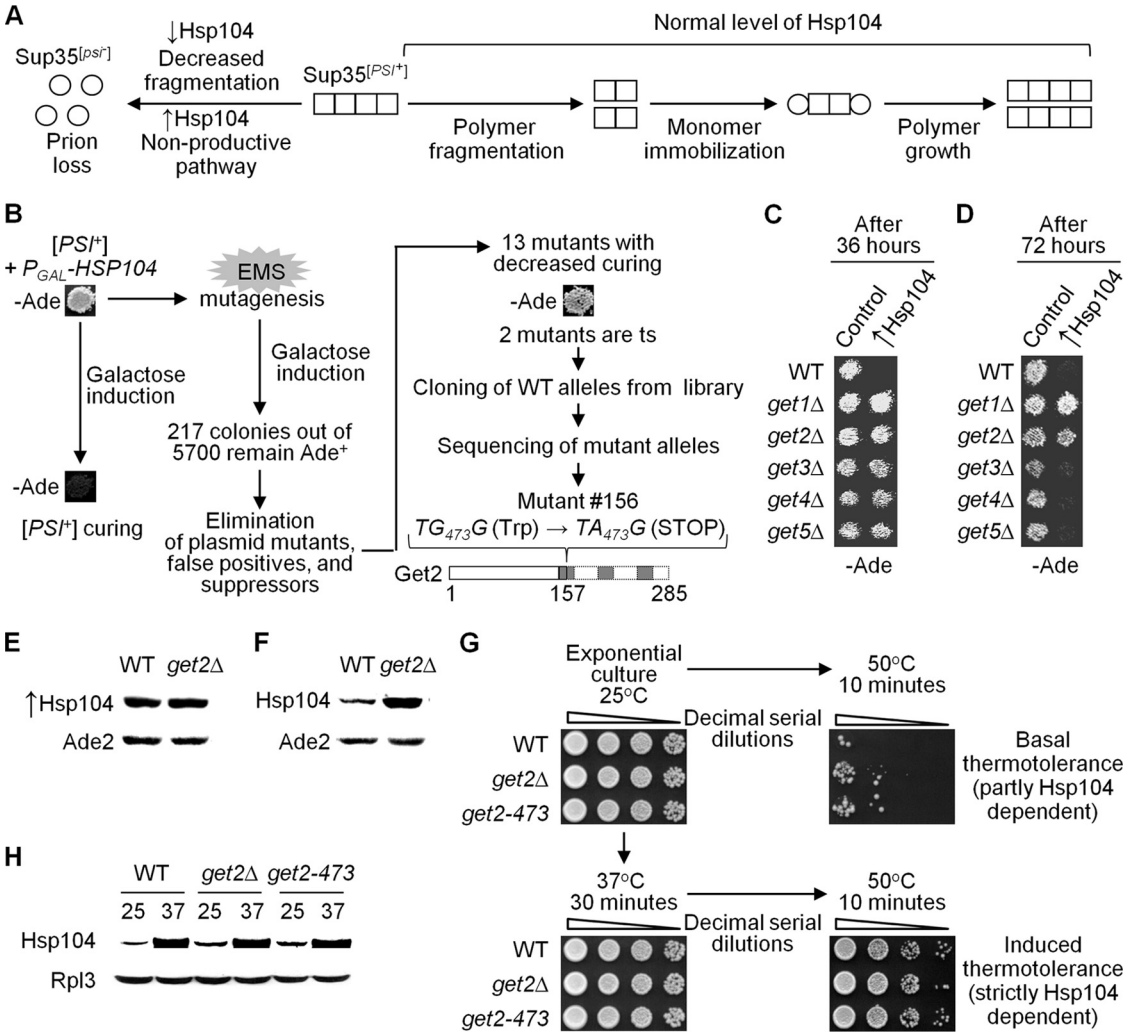


**FIG 1** *get* deficiencies impair [*PSI*$^+$] curing by excess Hsp104. (A) The known role of the chaperone Hsp104 in propagation of the [*PSI*$^+$] prion. At normal levels, Hsp104 promotes fragmentation of Sup35 polymers (composed of a prion isoform [squares]) into oligomers, initiating new rounds of prion propagation (right part of the panel). A decrease ( ↓ ) in Hsp104 levels (left part, upper portion) impairs oligomer production, leading to eventual loss ("curing") of prion polymers in future cell generations and to accumulation of newly synthesized Sup35 in a nonprion form (circles). An increase ( ↑ ) in Hsp104 levels (left part, bottom portion) directs Sup35 polymers to the "nonproductive" pathway, also resulting in prion curing and accumulation of a nonprion form of Sup35. (B) Screening for EMS-induced mutants defective in [*PSI*$^+$] curing by excess Hsp104. One of the curing-defective mutants (mutant 156) was complemented by a plasmid with the *GET2* gene. The initial mutation was identified as a G-to-A substitution at position 473 of the *GET2* gene (*get2-473*), resulting in a premature stop codon at amino acid position 157. This mutation prevents synthesis of the C-terminal part of the Get2 protein (dotted lines), thus eliminating 2.5 of 3 transmembrane domains (gray boxes). (C) Deletion of *GET1*, *-2*, *-3*, *-4*, or *-5* decreased [*PSI*$^+$] curing by excess Hsp104, similar to the *get2-473* mutation. [*PSI*$^+$] curing in the wild-type (WT) and *get*Δ cultures was detected by a decrease or elimination of growth on −Ade medium selective for $P_{GAL}$-*HSP104* following 36 h of induction on galactose. (D) The [*PSI*$^+$] curing defect was stronger in *get1*Δ and *get2*Δ strains than in the other *get*Δ strains. The same assay as that for panel C was performed after a longer (72 h) induction of $P_{GAL}$-*HSP104*. For panels C and D, plates were photographed after 4 days of incubation. (E) The *get2*Δ deletion did not change the level of Hsp104 produced from the plasmid-borne $P_{GAL}$-*HSP104* construct after 24 h. Cells were grown in −Ura medium with galactose and raffinose. Amounts of total protein were normalized by use of Ade2, as shown. Per the densitometry results, Hsp104 levels in the *get2*Δ strain were identical (with a standard error of ±0.1) to those in the wild-type (WT) strain. (F) The *get2*Δ deletion increased background levels of endogenous Hsp104 in mid-exponential-phase cultures grown in YPD medium. Amounts of total protein were normalized by use of Ade2. Per the densitometry results, Hsp104 levels in the *get2*Δ cells were 12- ± 0.9-fold higher than those in wild-type (WT) cells. Note that different exposures were used for panels E and F; therefore, Hsp104 levels should not be compared between the panels. (G) *GET2* alterations do not impair Hsp104's function in thermotolerance. Exponential-phase cultures of the strains with the *get2* deletion (*get2*Δ) or mutation (*get2-473*) exhibited increased basal tolerance (top right image) and similar induced tolerance (after pretreatment at 37°C) (bottom right image) to a 50°C heat shock compared to the wild-type (WT) strain. Nontreated cultures are shown on the left, as a control. Decimal serial dilutions were plated onto YPD plates and incubated for 4 days at 25°C in each case. (H) Levels of Hsp104 induced by incubation at 37°C for 30 min were the same (within a standard error of ±0.1, as confirmed by densitometry) in the WT, *get2*Δ, and *get2-473* strains. The ribosomal protein Rpl3 was used as a loading control.

Hsp104 levels in the absence of an overproducer plasmid were increased (about 10-fold or higher) rather than decreased in the *get2*Δ strain (Fig. 1F). Other *get* deletions also induced Hsp104 (see Fig. S1H in the supplemental material). Induced thermotolerance of an exponential-phase yeast culture to severe (50°C) heat shock after pretreatment at 37°C, a phenotype that is strictly dependent on Hsp104 (55), was not changed in the strains containing the *get2* deletion or mutation compared to the isogenic wild-

type strain (Fig. 1G). This is in good agreement with the observation that Hsp104 was induced to about the same level after a 37°C pretreatment in both wild-type and *get2*-defective strains (Fig. 1H). Notably, basal thermotolerance to 50°C (without pretreatment) was actually increased in the strains with *get* alterations, consistent with the increased basal Hsp104 levels in these strains. Thus, decreased [*PSI*$^+$] curing by excess Hsp104 in strains with *get* deficiencies is not due to a general impairment of Hsp104 function.

**Genetic interactions between *get* deficiencies and other alterations influencing [*PSI*$^+$] curing.** The chaperone proteins Hsp70-Ssa, Hsp70-Ssb, Hsp40-Sis1, and Hsp40-Ydj1, as well as Hsp90 with its cochaperones, Sti1 and Cpr7, and the ubiquitin-conjugating enzyme Ubc4, are known to influence effects of Hsp104 on [*PSI*$^+$] (reviewed in references 35 and 51). We checked for functional interactions between the respective genes and the *get2*Δ deletion in regard to [*PSI*$^+$] curing. Overproduction of Ssa1 (Fig. 2A) or Ydj1 (see Fig. S1B and C in the supplemental material) ameliorated [*PSI*$^+$] curing in the wild-type strain but did not have an effect on curing in the *get2*Δ strain, while excess Sis1 slightly increased [*PSI*$^+$] curing in both the *get2*Δ and wild-type strains (see Fig. S1D and E). An overproduction of Ssb1, known to increase [*PSI*$^+$] curing in the wild-type strain, also increased curing in the *get2*Δ strain (not shown), while the deletion of both Ssb-encoding genes, *ssb1/2*Δ, decreased curing only in the wild-type strain, not the *get2*Δ strain (Fig. 2B). This suggests that the Get2 and Hsp70 proteins influence [*PSI*$^+$] curing by excess Hsp104 through the same pathway, with Ssa and Ssb acting in opposite directions and Hsp40s possibly participating in the pathway as well.

Effects of *sti1* (Fig. 2C) or *cpr7* (Fig. 2D) deletion on [*PSI*$^+$] curing were additive to the effect of the *get2*Δ deletion. This shows that the action of *get* deficiencies on [*PSI*$^+$] is not mediated by Hsp90's cochaperones. Likewise, a combination of the *get2*Δ deletion with the *ubc4*Δ deletion (Fig. 2E) exhibited a stronger defect of [*PSI*$^+$] curing than that with either single deletion, indicating that the *get2*Δ deletion and defects of the ubiquitin-proteasome system are likely to affect [*PSI*$^+$] curing via different pathways.

Because *get* deficiencies lead to aggregation of cytosolic Get and TA proteins (57), one could suggest that Hsp104 sequestration by aggregates impairs the effect of excess Hsp104 on [*PSI*$^+$] curing. To test this possibility, we employed a construct containing the N-terminal region of the human huntingtin protein with an expanded (to 103 residues) polyglutamine stretch followed by a proline-rich region (103QP) and fusion to GFP. In yeast, aggregated 103QP is assembled into a perivacuolar (and typically perinuclear) deposit (67) resembling other quality control deposits of aggregated proteins, such as the mammalian aggresome (29) and yeast IPOD (27). Expression of 103QP-GFP did not inhibit [*PSI*$^+$] curing by excess Hsp104 (see Fig. S1F in the supplemental material), indicating that the effect of *get* deficiencies on [*PSI*$^+$] curing is not due to nonspecific sequestration of Hsp104 by protein aggregates.

**Deletion of *SGT2* ameliorates the [*PSI*$^+$] curing defect in *get*Δ strains.** In contrast to *get* deletions, a deletion of the gene coding for the cochaperone Sgt2, which is also associated with the GET pathway (see above), did not antagonize [*PSI*$^+$] curing by excess Hsp104 (Fig. 3A). Moreover, the *sgt2*Δ deletion ameliorated the [*PSI*$^+$] curing defect of each *get* deletion (Fig. 3A and B). The average size of the Sup35 prion aggregates, as determined by SDD-AGE, was somewhat increased in the *get2*Δ strain; this increase was eliminated by the *sgt2*Δ deletion (see Fig. S1G in the supplemental material). Weak [*PSI*$^+$] variants are known to be destabilized by a short-term (30 min) mild

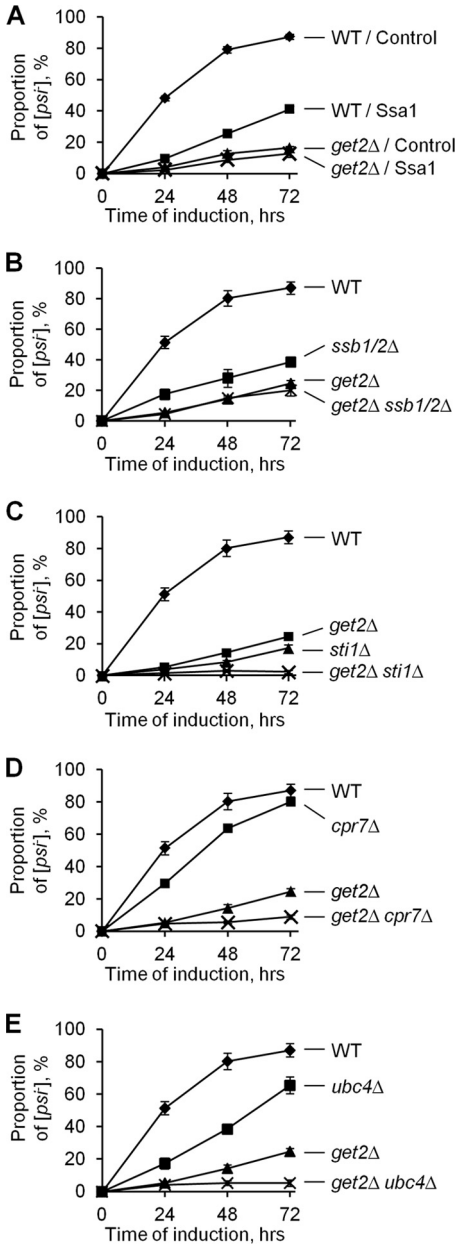


**FIG 2** Genetic interactions of the *get2*Δ deletion with other genes known to influence [*PSI*$^+$] curing. (A and B) Overproduction of Ssa1 (A) or deletion of both *SSB* genes (*ssb1/2*Δ) (B) antagonized [*PSI*$^+$] curing by excess Hsp104 in the Get$^+$ but not the *get2*Δ strain, thus revealing an epistatic interaction with the *get2*Δ deletion. (C to E) Deletion of *STI1* (C), *CPR7* (D), or *UBC4* (E) antagonized [*PSI*$^+$] curing by excess Hsp104 in both the wild-type and *get2*Δ strains, revealing an additive effect with the *get2*Δ deletion. In all experiments, cultures were grown in plasmid-selective medium with galactose and raffinose, and aliquots were taken and plated onto plasmid-selective medium with glucose after the specified periods. The presence or absence of [*PSI*$^+$] was detected after replica plating to −Ade medium. At least three experiments were performed for each culture. Standard deviations are shown by error bars. In cases where error bars are not seen, the standard deviation was smaller than the symbol. WT, wild type; control, empty vector.

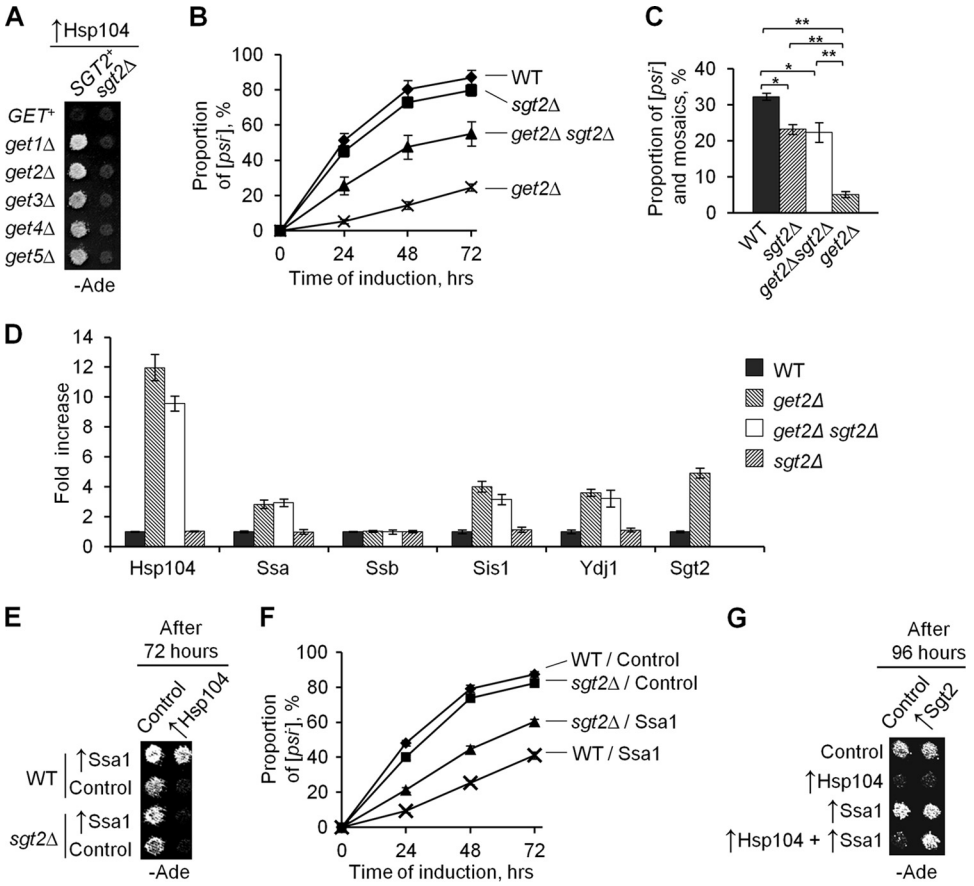


**FIG 3** Sgt2 aids Ssa in protecting [*PSI*$^+$] from curing by excess Hsp104. (A and B) Deletion of *SGT2* partly restored [*PSI*$^+$] curing by excess Hsp104 in the *get*Δ strains, as seen from both a plate assay of all *get* deletion strains (A) and a quantitative assay of *get2*Δ strains (B). Experiments were performed as described in the legend to Fig. 1B (for panel A) or Fig. 2 (for panel B). (C) [*PSI*$^+$] destabilization during short-term mild heat shock was significantly decreased by the *get2*Δ deletion, while the *sgt2*Δ deletion slightly decreased [*PSI*$^+$] destabilization in the Get$^+$ strain but almost restored it in the *get2*Δ strain. [*PSI*$^+$] destabilization was scored by color on YPD; complete [*psi*$^-$] and mosaic [*PSI*$^+$]/[*psi*$^-$] colonies were added together. Differences were concluded to be statistically significant at $P_{Ho}$ values of $<0.05$ (*) or $<0.01$ (**), according to the *t* test (40). No significant [*PSI*$^+$] loss was detected in the control cultures left at 25°C (not shown). (D) The stress response induced by *get2*Δ deletion was not ameliorated by *sgt2*Δ deletion. Protein levels, determined by densitometry of Western blots, are shown in relation to the wild-type strain level. Cultures were grown in YPD to the log phase. Ade2 was used as a loading control. (E) Deletion of *SGT2* decreased protection of [*PSI*$^+$] from excess Hsp104 by excess Ssa1 in the Get$^+$ strain (plate assay). After induction of Ssa1 and Hsp104 from the $P_{GAL}$ promoter on galactose medium, plates were replica plated onto −Ade medium selective for both plasmids. (F) Deletion of *SGT2* decreased protection of [*PSI*$^+$] from excess Hsp104 by excess Ssa1 in the Get$^+$ strain (quantitative assay). (G) Overproduction of Sgt2 increased [*PSI*$^+$] protection from excess Hsp104 by excess Ssa1. All constructs were induced from the $P_{GAL}$ promoter. The experiment was performed as described for panel E, except for the longer incubation period on galactose, as indicated. WT, wild type; control, respective empty vector. Plate images were taken after 3 (A and G) or 4 (E) days of incubation.

heat shock, possibly due to a more rapid accumulation of Hsp104 than of other Hsps (44). In agreement with these data, the *get2*Δ deletion reduced destabilization of the weak [*PSI*$^+$] variant by mild heat shock, while the *sgt2*Δ deletion reversed this effect (Fig. 3C).

**Induction of stress response by *get* deletions does not depend on Sgt2.** In addition to Hsp104, *get* deletions induced expression of other Hsps, specifically Hsp70-Ssa, Hsp40-Sis1, and Hsp40-Ydj1 (Fig. 3D; see Fig. S1H in the supplemental material). This is consistent with the previously reported induction of the general stress response in strains deficient in the GET pathway (5). As expected, levels of Hsp70-Ssb, which is not stress inducible, were not changed. Notably, Sgt2 levels were increased in the strains with *get* deletions. However, the *sgt2*Δ deletion did not affect Hsp induction in the *get*-deficient strains (Fig. 3D; see Fig. S1H), indicating that induction of the stress response by *get* alterations is independent of Sgt2.

**Sgt2 is involved in protection of [*PSI*$^+$] from excess Hsp104 by excess Ssa.** Increased levels of Ssa in *get* deletion strains could provide the simplest explanation for the effect of *get* deficiencies on [*PSI*$^+$] curing, as Ssa is known to reverse the effect of excess Hsp104 on [*PSI*$^+$] (45). However, restoration of [*PSI*$^+$] curing by the *sgt2*Δ deletion without affecting Ssa levels indicates that Sgt2 is needed for efficient [*PSI*$^+$] protection by excess Ssa. To test this further, we compared the effects of Ssa1 and Hsp104 overproduction in Get$^+$ [*PSI*$^+$] strains that differed from each other by the presence, absence, or overproduction of Sgt2. Indeed, the *sgt2*Δ deletion interfered with the ability of excess Ssa1 to protect [*PSI*$^+$] from excess Hsp104. This effect was clearly seen in the plate assay (Fig. 3E). Differences were also statistically significant in the quantitative assay in liquid medium, although the *sgt2*Δ deletion did not completely abolish [*PSI*$^+$] protection by excess Ssa (Fig. 3F). Levels of the Hsp104 and Ssa proteins, induced from the $P_{GAL}$ promoter, were not affected by the *sgt2*Δ deletion, confirming that

the decrease in the protective effect of Ssa on curing was not due to a change in chaperone accumulation (data not shown). Sgt2 overproduction did not have any effect on [*PSI*$^+$] mitotic stability (not shown) or on [*PSI*$^+$] curing by excess Hsp104 on its own; however, it increased [*PSI*$^+$] protection from excess Hsp104 in the presence of excess Ssa (Fig. 3G).

Taken together, our data indicate that the defect in [*PSI*$^+$] curing by excess Hsp104 in the strains with *get* alterations was due to simultaneously increased levels of both Ssa and Sgt2. The residual ability of excess Ssa to protect [*PSI*$^+$] from excess Hsp104 in the absence of Sgt2 (Fig. 3F) explains why the *sgt2*Δ deletion did not completely abolish [*PSI*$^+$] protection in the *get2*Δ strain (Fig. 3B).

**Role of Sgt2 in the other phenotypes caused by *get* deletions.** The *sgt2*Δ deletion partly ameliorated the antibiotic sensitivities of *get1*, *get2*, and *get3* deletion strains but did not have any effect on temperature sensitivity (an example with the *get2*Δ strain is shown in Fig. S1I in the supplemental material). When the GET pathway is disrupted, the cytosolic Get proteins and TA proteins form cytologically detectable aggregates in the cytoplasm (57). We confirmed the coaggregation of the Sgt2, Get3 (Fig. 4A), Get5 (see Fig. S2A in the supplemental material), and Get4 (data not shown) proteins within the same clumps in the *get2*Δ cells. We have also shown that cytoplasmic Get aggregates (visualized by tagged Get3) colocalize with neither Dcp2 (Fig. 4B) and Edc3 (see Fig. S2B), which are markers of P-bodies (9, 16), nor Pub1 (Fig. 4C), a marker of stress granules (9). Thus, Get-TA aggregates are distinct from other known cytoplasmic assemblies. Aggregation of Get3 (Fig. 4D and E), Get4 (see Fig. S2C), and Get5 (see Fig. S2D) in the *get2*Δ cells strictly depended on the presence of Sgt2, in agreement with a model suggesting that Sgt2 participates in linking the cytosolic Get proteins to TA proteins, and possibly to chaperones (65). Formation of Get aggregates was abolished (see Fig. S2E) in the presence of benomyl, an inhibitor of microtubule assembly in yeast (28). This suggests a direct or indirect dependence of Get-TA aggregate formation on the microtubular cytoskeleton, as demonstrated previously (67) and confirmed here (see Fig. S2F) for the aggresome-like deposits of 103QP in yeast. The TA protein Sbh1, a component of the Sec61 translocon complex normally localized to the ER membrane (63), was mislocalized and coaggregated with Get3 in the same *get2*Δ strain; notably, the *sgt2*Δ deletion restored the membrane localization of Sbh1 (Fig. 4F). Thus, some (though not all) phenotypes of *get* deletions depend on the presence of Sgt2.

**Effects of prions on Sgt2 levels.** The [*PSI*$^+$] prion was previously reported to induce Hsps (18, 58); however, these data were obtained with strains also containing the tRNA suppressor gene *SUP16* (*SUQ5*), which further increases translational readthrough. In our strains, the presence of neither [*PSI*$^+$] nor [*PIN*$^+$] prions increased the level of Hsp104, Ssa, or Sis1 (Fig. 5A). Remarkably, the presence of both [*PSI*$^+$] and [*PIN*$^+$] simultaneously or [*PIN*$^+$] alone led to a 4-fold or 2-fold increase, respectively, in the levels of Sgt2 in the same strains compared to the [*psi*$^-$ *pin*$^-$] control (Fig. 5B). These data show that the Sgt2 level serves as a more sensitive detector of amyloid presence than Hsp levels, with different prions exhibiting additive effects on the accumulation of Sgt2.

**Physical interactions between Sgt2 and prion/amyloid proteins.** A large-scale two-hybrid assay previously detected an interaction between Sgt2 and Rnq1 (70). We checked to see if Sgt2 interacts with Sup35. Indeed, a two-hybrid assay demonstrated that Sgt2 and the N-terminal (prion) domain of Sup35, Sup35N, interact with each other (Fig. 5C). Sgt2 also interacted with itself, confirming previous reports that it is a homodimer (10). The C-terminal domain of Sgt2 (amino acids 221 to 346), known to interact with the hydrophobic tails of TA proteins (65), was required for the two-hybrid interaction with Sup35N, while the N-terminal

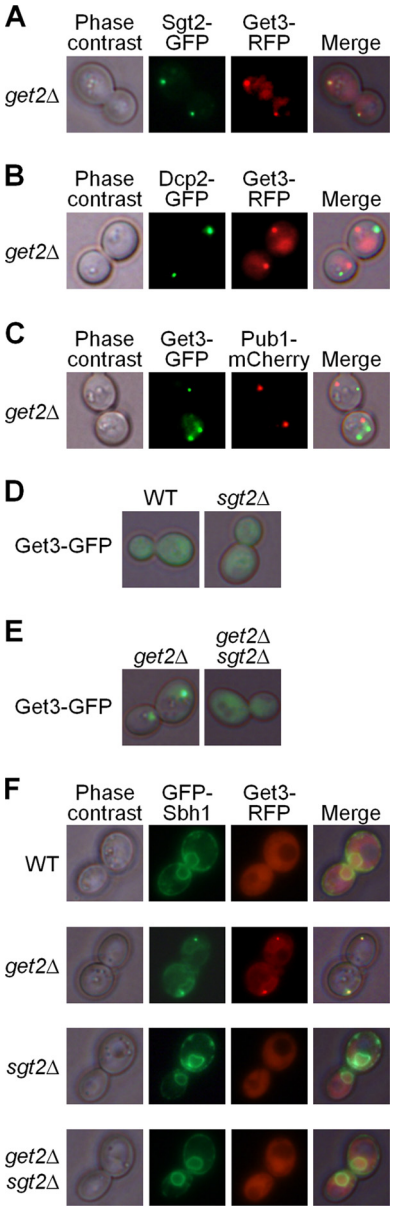


**FIG 4** Aggregation patterns in strains with the *get2*Δ and/or *sgt2*Δ deletion. (A) In the *get2*Δ strain, Get3 (tagged by red fluorescent protein [RFP]) and Sgt2 (tagged by GFP) formed aggregates that were colocalized. (B and C) Get-TA aggregates, marked by fluorescently tagged Get3, did not colocalize with the P-body marker Dcp2 (B) or with the stress granule marker Pub1 (C). (D) The *sgt2*Δ deletion did not cause the formation of Get-TA aggregates (marked by Get3-GFP) in the Get$^+$ strain. (E) The *sgt2*Δ deletion abolished aggregation of the cytosolic Get protein Get3-GFP in the *get2*Δ strains. (F) The tail-anchored protein Sbh1 (tagged by GFP) was localized to the endoplasmic reticulum membrane in the wild-type (WT) strain but was colocalized with the Get3 aggregates in the *get2*Δ strain. Membrane localization of Sbh1 was not altered by the *sgt2*Δ deletion and was restored in the *get2*Δ *sgt2*Δ strain.

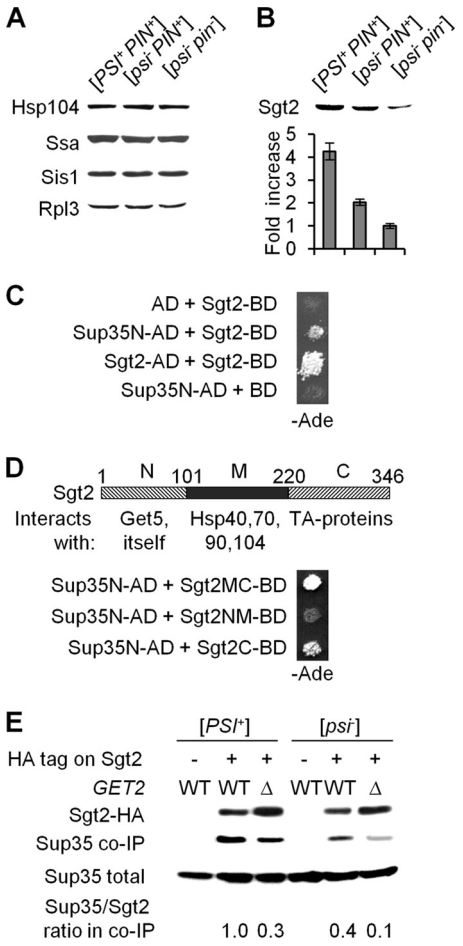


**FIG 5** Physical interactions of Sgt2 with amyloidogenic proteins. (A and B) The presence of [*PSI*$^+$] and/or [*PIN*$^+$] prions did not increase levels of major Hsps in our strains (A); however, it did increase levels of Sgt2, in an additive fashion (B). Rpl3 served as a loading control. Densitometry data in panel B are shown in relation to the [*psi*$^-$ *pin*$^-$] strain. Average results for three independent experiments are shown. For each pairwise combination, the difference is statistically significant. (C) Sgt2 interacts with the prion domain of Sup35 (Sup35N) and with itself in the two-hybrid assay. (D) Known information about the protein interaction capabilities of the Sgt2 domains (shown on the scheme) is compared to the abilities of these domains to interact with Sup35N in the two-hybrid assay. Numbers over the Sgt2 map indicate amino acid positions. In both panels C and D, two-hybrid interaction was detected by activation of the $P_{GAL2}$-*ADE2* reporter, resulting in growth on −Ade medium. Plate images were taken after 5 days of incubation. (E) Sup35 is coimmunoprecipitated with HA-tagged Sgt2. The absence or presence of the HA tag in the chromosomal copy of the *SGT2* gene is indicated with "−" or "+," respectively. Anti-HA antibodies were used to precipitate Sgt2-HA. Coimmunoprecipitated Sup35 was detected in the samples prepared from *SGT2-HA* strains but not in the samples prepared from strains with nontagged *SGT2*. Levels of Sgt2-associated Sup35 were determined by densitometry, using Sup35 in total lysate as a loading control, and are shown in relation to the strain with the highest level, whose level was considered 1.0.

domain of Sgt2 (amino acids 2 to 101), known to interact with Get5 (10, 65), was dispensable for the interaction with Sup35N (Fig. 5D). The middle (M) domain of Sgt2 (amino acids 102 to 220), previously implicated in interactions with Hsps (10, 65), was not sufficient for a two-hybrid interaction with Sup35N; however, the presence of this domain increased the interaction.

Co-IP experiments also confirmed an interaction between HA-tagged Sgt2 (used as "bait") and Sup35 (Fig. 5E). Co-IP was detected in both [*PSI*$^+$] and [*psi*$^-$] cells; however, it was more efficient in [*PSI*$^+$] cells if normalized by the amount of precipitated Sgt2-HA. This indicates a higher affinity of Sgt2 for the prion form of Sup35 or could have resulted from higher Sgt2 levels in the [*PSI*$^+$] strains. The latter possibility seems likely, as a 2-fold difference in Sgt2 levels between the [*PSI*$^+$ *PIN*$^+$] and [*psi*$^-$ *PIN*$^+$] strains correlates well with an approximately 2.5-fold difference in the amounts of Sup35 coprecipitated with Sgt2 from these strains. Likewise, the ratio of coimmunoprecipitated Sup35 to Sgt2 was decreased in the *get2*Δ background, where Sgt2 levels were increased. Apparently, in cells lacking Get2, much of the excess Sgt2 was targeted to cytosolic Get-TA aggregates. Notably, Sup35 prion aggregates (marked by Sup35-dsRed) were colocalized with the Get-TA aggregates (marked by Get3-GFP or Sgt2-GFP) in 12 to 15% of the [*PSI*$^+$] cells that exhibited Get-TA aggregate formation (see Fig. S2G and H in the supplemental material). This confirms at least an occasional association between these two types of aggregated structures, possibly mediated via Sgt2 and maybe reflecting an Sgt2-Sup35 interaction occurring in the *get2*Δ cells.

Previous works (66, 67) indicated that Sgt2 is associated with polyglutamines expressed in yeast cells containing an endogenous prion. We showed that about 8% of wild-type cells with no genetic disruption of the GET pathway but expressing 103QP-GFP and containing aggresome-like 103QP deposits (67) also contained Get3 clumps. Moreover, the Get3 clumps were always located next to (or partly overlapping) the 103QP-GFP deposit, indicating that polyglutamines nucleate aggregation of the Get3 protein in Get$^+$ cells (see Fig. S2I in the supplemental material). In about 12% of the *get2*Δ cells bearing both 103QP-RFP and Sgt2-GFP aggregates, these aggregates were colocalized or juxtaposed with each other (see Fig. S2J). This points to an interaction between the quality control compartments containing amyloid-like aggregates and cytosolic Get (and possibly TA) proteins, presumably occurring via Sgt2.

## DISCUSSION

Our data demonstrate that disruption of the GET pathway protects the prion [*PSI*$^+$] from excess chaperone Hsp104 via inducing the chaperone Hsp70-Ssa and the cochaperone Sgt2. Moreover, Sgt2 also modulates the actions of Ssa and Hsp104 on [*PSI*$^+$] in strains with a normally functioning GET pathway. Notably, Sgt2 does not have a noticeable effect on [*PSI*$^+$] on its own, and its abundance becomes important for a prion only when Ssa is present in excess.

A postulated function of Sgt2 in the GET pathway is targeting of Hsps and cytoplasmic Get proteins to the newly synthesized TA proteins (10, 65). This ensures protection of the hydrophobic tails of TA proteins from intermolecular collapse. Interestingly, our data show that disruption of TA trafficking in cells with a defective GET pathway depends on Sgt2. Cytosolic Get proteins, TA proteins, and Sgt2 form aggregates in the cytoplasm of *get2*Δ cells (57) (Fig. 4). However, in a strain lacking both Get2 and Sgt2, the aggregation of Get proteins (Fig. 4E; see Fig. S2C and D in the supplemental material) and the TA protein Sbh1 (Fig. 4F) is abolished, and localization of Sbh1 to the ER membrane is restored. This shows that in GET-deficient cells lacking Sgt2, at least some TA proteins are not sequestered into aggregates, allowing trafficking via an alternative pathway, whose existence was proposed previously (48, 57). It is possible that such an alternative pathway utilizes Hsp70 and Hsp40 chaperones, which have been shown to

facilitate *in vitro* integration of TA proteins into membranes (1, 50). This is consistent with the high levels of Hsp induction observed in the *get*Δ and *get*Δ *sgt2*Δ strains (Fig. 3D; see Fig. S1H in the supplemental material) and with the role of Sgt2 as a chaperone targeting factor.

Our data indicate that Sgt2 also plays a role in targeting Hsps (specifically Ssa) to prion aggregates. Sgt2 is known to interact with Hsps (10, 65) and with the prion protein Rnq1 (70), and our data uncovered an interaction of Sgt2 with the prion protein Sup35 (Fig. 5). Sgt2 was also detected among the proteins associated with polyglutamine aggregates in yeast cells (66, 67). Remarkably, one (C-terminal) domain of Sgt2 is involved in binding both hydrophobic tails of TA proteins and the prion domain of Sup35 (Fig. 5D). This suggests that the cellular function of Sgt2 is not confined to the GET pathway. Rather, Sgt2 targets chaperones to different types of aggregation-prone proteins. Indeed, Sgt2 manifests itself as a sensitive indicator of the presence of amyloid-based prions in the yeast cell, as its levels are increased in the presence of a prion(s) under conditions where conventional Hsps are not induced (Fig. 5A and B). A decrease in the proportion of Sgt2-associated Sup35 in *get2*Δ cells, in which Get-TA aggregates are formed (Fig. 5E), indicates that different types of aggregation-prone proteins compete for Sgt2 binding. However, occasional colocalization of Sup35 prion aggregates and cytosolic Get-TA aggregates (see Fig. S2G and H in the supplemental material), as well as occasional nucleation of the Get-TA aggregates by the polyglutamine-derived quality control deposits (see Fig. S2I), points to the possibility of Sgt2 linking different aggregated proteins to each other, thus forming more complex assemblies. Whether this plays a role in detoxification and/or elimination of aggregated proteins remains to be seen. However, taking into account that Get-TA aggregate formation depends on the microtubular cytoskeleton (see Fig. S2E) and that Sgt2 is involved in stress resistance (4), the possibility of Sgt2 triggering the specific assembly pathway that counteracts potential cytotoxicity of aggregation-prone proteins appears to be quite likely.

It is not yet entirely clear how excess Ssa reverses the effect of excess Hsp104 on [*PSI*$^+$]; therefore, a molecular basis for the role of Sgt2 in this process remains hypothetical (Fig. 6). It has been proposed (35) that the proper balance between Ssa and Hsp104, rather than an intermediate level of Hsp104 *per se*, is required for the efficient fragmentation (and therefore propagation) of Sup35 prion aggregates. Indeed, recent experiments in various models indicated that aggregate fragmentation is initiated by Hsp70 (bacterial DnaK) and/or its Hsp40 cochaperone (bacterial DnaJ or yeast Sis1), while Hsp104 acts on further stages (69). In the case where Hsp104 is present in excess, it might interact with the aggregates without Ssa. Such a "nonproductive" interaction would not result in an efficient fragmentation of prion aggregates to oligomers. Analysis of [*PSI*$^+$] loss after short-term heat shock (that is, also under conditions of Hsp104-Ssa imbalance) suggests that prion interaction with excess Hsp104 may lead to asymmetric accumulation of prion aggregates in the mother cell, and eventually to segregational loss of a prion (44). When both Ssa and Hsp104 are present in excess, the proper chaperone balance, and therefore proper fragmentation, is restored. However, this occurs only if Ssa has unrestricted access to Sup35 aggregates. In such a scenario, the role of Sgt2 would be to target excess Ssa to the prion. This could be achieved via promoting Ssa binding to an amyloid substrate and/or altering the structural parameters of amyloid aggregates, thus making them more accessible to Ssa. Modulation of the Hsp104 interaction with either Ssa or aggregates (or both) by Sgt2 also cannot be excluded. Further experiments aimed at determining which of these interactions provide a major input(s) into the observed outcomes are under way.

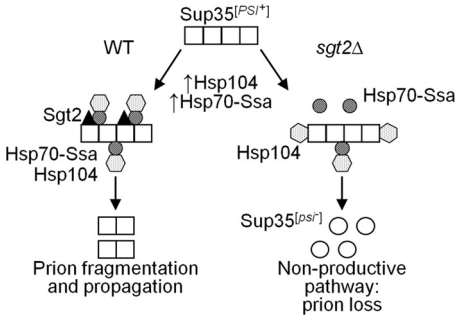


**FIG 6** Model for the effects of Sgt2 and Hsp70-Ssa on [*PSI*$^+$] curing by excess Hsp104. Hsp104 (dotted hexagons) promotes fragmentation of Sup35 prion polymers (squares) by binding them via the chaperone Hsp70-Ssa (striped circles). However, excess Hsp104 binds prion polymers on its own (without Hsp70-Ssa) at different sites and impairs prion propagation. In the *sgt2*Δ strain (right panel), overproduction of Hsp70-Ssa does not significantly increase the amount of polymer-bound Hsp70-Ssa, as the number of accessible sites is limited. However, when Sgt2 is present (left panel), it increases access of Hsp70-Ssa to prion polymers. This results in targeting of excess Hsp104 to polymer-bound Hsp70-Ssa and therefore in restoration of normal prion fragmentation and propagation. Some Hsp40 chaperones (not shown in the figure) serve as cochaperones of Hsp70-Ssa, and Hsp70-Ssb presumably antagonizes Hsp70-Ssa. Effects of disruptions of the GET pathway are due to induction of Hsps and Sgt2.

Taking into account that *get* disruption affects [*PSI*$^+$] via Sgt2 and Ssa actions, one may draw additional interesting conclusions from the genetic interactions between *get* deletions and alterations of some other chaperone/cochaperone proteins in regard to their effects on [*PSI*$^+$]. For example, the epistatic interaction between the double *ssb1/2* deletion and the *get2*Δ deletion (Fig. 2B) suggests that Ssb might act on [*PSI*$^+$] via antagonizing, directly or indirectly, the interaction of Ssa with prion aggregates. On the other hand, additive genetic interactions between the *get2*Δ deletion and deletions of the genes coding for the Hsp90/70 cochaperones Sti1 and Cpr7 (Fig. 2C and D) indicate that these cochaperones (and possibly their interacting partner, Hsp90) assist Hsp104 in [*PSI*$^+$] curing via a mechanism that does not include direct competition with Ssa.

Since an Sgt2 ortholog is conserved across eukaryotes, including humans (30), the question of whether human Sgt2 has any effect on amyloids associated with human aggregation disorders arises. The intimate relationship between Sgt2 and the chaperone machinery that controls amyloid propagation in yeast makes Sgt2 involvement in human amyloidoses an attractive topic for further investigations.

## ACKNOWLEDGMENTS

We thank R. Brazas, E. Craig, D. Cyr, S. Elledge, P. Hieter, S. Lindquist, R. Parker, M. Schuldiner, and J. Warner for plasmids and antibodies, Y. Nishida and A. Romanyuk for help with some experiments, K. Bruce and G. Newnam for proofreading the manuscript, Y. Pavlov for guidance on the EMS mutagenesis experiments, and J. Weissman for helpful discussions.

This work was supported by grants R01GM058763 and R01GM093294

from the NIH. J.C.P. was supported by an undergraduate research scholarship from the Institute for Bioengineering and Bioscience.

The content of this paper is solely the responsibility of the authors and does not necessarily represent the official views of the NIH.

## REFERENCES

1. **Abell BM, Rabu C, Leznicki P, Young JC, High S.** 2007. Post-translational integration of tail-anchored proteins is facilitated by defined molecular chaperones. J. Cell Sci. **15**:1743–1751.
2. **Allen KD, Chernova TA, Tennant EP, Wilkinson KD, Chernoff YO.** 2007. Effects of ubiquitin system alterations on the formation and loss of a yeast prion. J. Biol. Chem. **282**:3004–3013.
3. **Allen KD, et al.** 2005. Hsp70 chaperones as modulators of prion life cycle: novel effects of Ssa and Ssb on the *Saccharomyces cerevisiae* prion [*PSI*$^+$]. Genetics **169**:1227–1242.
4. **Angeletti PC, Walker D, Panganiban AT.** 2002. Small glutamine-rich protein/viral protein U-binding protein is a novel cochaperone that affects heat shock protein 70 activity. Cell Stress Chaperones **7**:258–268.
5. **Auld KL, et al.** 2006. The conserved ATPase Get3/Arr4 modulates the activity of membrane-associated proteins in *Saccharomyces cerevisiae*. Genetics **174**:215–227.
6. **Bailleul PA, Newnam GP, Steenbergen JN, Chernoff YO.** 1999. Genetic study of interactions between the cytoskeletal assembly protein sla1 and prion-forming domain of the release factor Sup35 (eRF3) in *Saccharomyces cerevisiae*. Genetics **153**:81–94.
7. **Bonneaud N, et al.** 1991. A family of low and high copy replicative, integrative and single-stranded *S. cerevisiae*/*E. coli* shuttle vectors. Yeast **7**:609–615.
8. **Borgese N, Brambillasca S, Colombo S.** 2007. How tails guide tail-anchored proteins to their destinations. Curr. Opin. Cell Biol. **19**:368–375.
9. **Buchan JR, Muhlrad D, Parker R.** 2008. P bodies promote stress granule assembly in *Saccharomyces cerevisiae*. J. Cell Biol. **183**:441–455.
10. **Chartron JW, Gonzalez GM, Clemons WM, Jr.** 2011. A structural model of the Sgt2 protein and its interactions with chaperones and the Get4/Get5 complex. J. Biol. Chem. **286**:34325–34334.
11. **Chernoff YO, et al.** 2000. Evolutionary conservation of prion-forming abilities of the yeast Sup35 protein. Mol. Microbiol. **35**:865–876.
12. **Chernoff YO, Lindquist SL, Ono B, Inge-Vechtomov SG, Liebman SW.** 1995. Role of the chaperone protein Hsp104 in propagation of the yeast prion-like factor [*psi*$^+$]. Science **268**:880–884.
13. **Chernoff YO, Newnam GP, Kumar J, Allen K, Zink AD.** 1999. Evidence for a protein mutator in yeast: role of the Hsp70-related chaperone ssb in formation, stability, and toxicity of the [*PSI*] prion. Mol. Cell. Biol. **19**:8103–8112.
14. **Chernoff YO, Uptain SM, Lindquist SL.** 2002. Analysis of prion factors in yeast. Methods Enzymol. **351**:499–538.
15. **Colby DW, Prusiner SB.** 2011. Prions. Cold Spring Harb. Perspect. Biol. **3**:a006833.
16. **Coller J, Parker R.** 2005. General translational repression by activators of mRNA decapping. Cell **122**:875–886.
17. **Durfee T, et al.** 1993. The retinoblastoma protein associates with the protein phosphatase type 1 catalytic subunit. Genes Dev. **7**:555–569.
18. **Eaglestone SS, Cox BS, Tuite MF.** 1999. Translation termination efficiency can be regulated in Saccharomyces cerevisiae by environmental stress through a prion-mediated mechanism. EMBO J. **18**:1974–1981.
19. **Eisenberg D, Jucker M.** 2012. The amyloid state of proteins in human diseases. Cell **148**:1188–1203.
20. **Fan CY, Lee S, Ren HY, Cyr DM.** 2004. Exchangeable chaperone modules contribute to specification of type I and type II Hsp40 cellular function. Mol. Biol. Cell **15**:761–773.
21. **Gerring SL, Spencer F, Hieter P.** 1990. The *CHL1* (*CTF1*) gene product of *Saccharomyces cerevisiae* is important for chromosome transmission and normal cell cycle progression in G2/M. EMBO J. **9**:4347–4358.
22. **Glover JR, Lindquist S.** 1998. Hsp104, Hsp70, and Hsp40: a novel chaperone system that rescues previously aggregated proteins. Cell **94**:73–82.
23. **Halfmann R, et al.** 2012. Prions are a common mechanism for phenotypic inheritance in wild yeasts. Nature **482**:363–368.
24. **James P, Halladay J, Craig EA.** 1996. Genomic libraries and a host strain designed for highly efficient two-hybrid selection in yeast. Genetics **144**:1425–1436.
25. **Janke C, et al.** 2004. A versatile toolbox for PCR-based tagging of yeast genes: new fluorescent proteins, more markers and promoter substitution cassettes. Yeast **21**:947–962.
26. **Jonikas MC, et al.** 2009. Comprehensive characterization of genes required for protein folding in the endoplasmic reticulum. Science **323**:1693–1697.
27. **Kaganovich D, Kopito R, Frydman J.** 2008. Misfolded proteins partition between two distinct quality control compartments. Nature **454**:1088–1095.
28. **Kilmartin JV.** 1981. Purification of yeast tubulin by self-assembly in vitro. Biochemistry **20**:3629–3633.
29. **Kopito RR.** 2000. Aggresomes, inclusion bodies and protein aggregation. Trends Cell Biol. **10**:524–530.
30. **Kordes E, et al.** 1998. Isolation and characterization of human SGT and identification of homologues in Saccharomyces cerevisiae and Caenorhabditis elegans. Genomics **52**:90–94.
31. **Kryndushkin DS, Alexandrov IM, Ter-Avanesyan MD, Kushnirov VV.** 2003. Yeast [*PSI*$^+$] prion aggregates are formed by small Sup35 polymers fragmented by Hsp104. J. Biol. Chem. **278**:49636–49643.
32. **Kushnirov VV, Ter-Avanesyan MD.** 1998. Structure and replication of yeast prions. Cell **94**:13–16.
33. **Lee S, Fan CY, Younger JM, Ren H, Cyr DM.** 2002. Identification of essential residues in the type II Hsp40 Sis1 that function in polypeptide binding. J. Biol. Chem. **277**:21675–21682.
34. **Lee SJ, Lim HS, Masliah E, Lee HJ.** 2011. Protein aggregate spreading in neurodegenerative diseases: problems and perspectives. Neurosci. Res. **70**:339–348.
35. **Liebman SW, Chernoff YO.** 2012. Prions in yeast. Genetics **191**:1041–1072.
36. **Liou ST, Cheng MY, Wang C.** 2007. *SGT2* and *MDY2* interact with molecular chaperone *YDJ1* in *Saccharomyces cerevisiae*. Cell Stress Chaperones **12**:59–70.
37. **Liu H, Krizek J, Bretscher A.** 1992. Construction of a *GAL1*-regulated yeast cDNA expression library and its application to the identification of genes whose overexpression causes lethality in yeast. Genetics **132**:665–673.
38. **Longtine MS, et al.** 1998. Additional modules for versatile and economical PCR-based gene deletion and modification in *Saccharomyces cerevisiae*. Yeast **14**:953–961.
39. **Maclea KS, Ross ED.** 2011. Strategies for identifying new prions in yeast. Prion **5**:263–268.
40. **McDonald JH.** 2009. Handbook of biological statistics, 2nd ed, p 118–122. Sparky House Publishing, Baltimore, MD.
41. **McGlinchey RP, Kryndushkin D, Wickner RB.** 2011. Suicidal [*PSI*$^+$] is a lethal yeast prion. Proc. Natl. Acad. Sci. U. S. A. **108**:5337–5341.
42. **Meriin AB, et al.** 2007. Endocytosis machinery is involved in aggregation of proteins with expanded polyglutamine domains. FASEB J. **21**:1915–1925.
43. **Moosavi B, Wongwigkarn J, Tuite MF.** 2010. Hsp70/Hsp90 co-chaperones are required for efficient Hsp104-mediated elimination of the yeast [*PSI*$^+$] prion but not for prion propagation. Yeast **27**:167–179.
44. **Newnam GP, Birchmore JL, Chernoff YO.** 2011. Destabilization and recovery of a yeast prion after mild heat shock. J. Mol. Biol. **408**:432–448.
45. **Newnam GP, Wegrzyn RD, Lindquist SL, Chernoff YO.** 1999. Antagonistic interactions between yeast chaperones Hsp104 and Hsp70 in prion curing. Mol. Cell. Biol. **19**:1325–1333.
46. **Ohba M.** 1997. Modulation of intracellular protein degradation by SSB1-SIS1 chaperon system in yeast *S. cerevisiae*. FEBS Lett. **409**:307–311.
47. **Prusiner SB.** 1982. Novel proteinaceous infectious particles cause scrapie. Science **216**:136–144.
48. **Rabu C, High S.** 2007. Membrane protein chaperones: a new twist in the tail? Curr. Biol. **17**:R472–R474.
49. **Rabu C, Schmid V, Schwappach B, High S.** 2009. Biogenesis of tail-anchored proteins: the beginning for the end? J. Cell Sci. **122**:3605–3612.
50. **Rabu C, Wipf P, Brodsky JL, High S.** 2008. A precursor-specific role for Hsp40/Hsc70 during tail-anchored protein integration at the endoplasmic reticulum. J. Biol. Chem. **283**:27504–27513.
51. **Reidy M, Masison DC.** 2011. Modulation and elimination of yeast prions by protein chaperones and co-chaperones. Prion **5**:245–249.
52. **Reidy M, Masison DC.** 2010. Sti1 regulation of Hsp70 and Hsp90 is critical for curing of *Saccharomyces cerevisiae* [*PSI*$^+$] prions by Hsp104. Mol. Cell. Biol. **30**:3542–3552.
53. **Rikhvanov EG, Romanova NV, Chernoff YO.** 2007. Chaperone effects on prion and nonprion aggregates. Prion **1**:217–222.

54. **Romanova NV, Chernoff YO.** 2009. Hsp104 and prion propagation. Protein Pept. Lett. **16**:598–605.
55. **Sanchez Y, Lindquist SL.** 1990. HSP104 required for induced thermotolerance. Science **248**:1112–1115.
56. **Sanchez Y, et al.** 1993. Genetic evidence for a functional relationship between Hsp104 and Hsp70. J. Bacteriol. **175**:6484–6491.
57. **Schuldiner M, et al.** 2008. The GET complex mediates insertion of tail-anchored proteins into the ER membrane. Cell **134**:634–645.
58. **Schwimmer C, Masison DC.** 2002. Antagonistic interactions between yeast [*PSI*$^+$] and [*URE3*] prions and curing of [*URE3*] by Hsp70 protein chaperone Ssa1p but not by Ssa2p. Mol. Cell. Biol. **22**:3590–3598.
59. **Serio TR, Cashikar AG, Moslehi JJ, Kowal AS, Lindquist SL.** 1999. Yeast prion [*psi*$^+$] and its determinant, Sup35p. Methods Enzymol. **309**:649–673.
60. **Shen J, Hsu CM, Kang BK, Rosen BP, Bhattacharjee H.** 2003. The Saccharomyces cerevisiae Arr4p is involved in metal and heat tolerance. Biometals **16**:369–378.
61. **Sherman F.** 2002. Getting started with yeast. Methods Enzymol. **350**: 3–41.
62. **Sikorski RS, Hieter P.** 1989. A system of shuttle vectors and yeast host strains designed for efficient manipulation of DNA in *Saccharomyces cerevisiae*. Genetics **122**:19–27.
63. **Toikkanen J, et al.** 1996. Yeast protein translocation complex: isolation of two genes *SEB1* and *SEB2* encoding proteins homologous to the Sec61β subunit. Yeast **12**:425–438.
64. **Vilardell J, Warner JR.** 1997. Ribosomal protein L32 of *Saccharomyces cerevisiae* influences both the splicing of its own transcript and the processing of rRNA. Mol. Cell. Biol. **17**:1959–1965.
65. **Wang F, Brown EC, Mak G, Zhuang J, Denic V.** 2010. A chaperone cascade sorts proteins for posttranslational membrane insertion into the endoplasmic reticulum. Mol. Cell **40**:159–171.
66. **Wang Y, Meriin AB, Costello CE, Sherman MY.** 2007. Characterization of proteins associated with polyglutamine aggregates: a novel approach towards isolation of aggregates from protein conformation disorders. Prion **1**:128–135.
67. **Wang Y, et al.** 2009. Abnormal proteins can form aggresome in yeast: aggresome-targeting signals and components of the machinery. FASEB J. **23**:451–463.
68. **Wickner RB, Edskes HK, Bateman D, Kelly AC, Gorkovskiy A.** 2011. The yeast prions [PSI+] and [URE3] are molecular degenerative diseases. Prion **5**:258–262.
69. **Winkler J, Tyedmers J, Bukau B, Mogk A.** 2012. Chaperone networks in protein disaggregation and prion propagation. J. Struct. Biol. **179**:152–160.
70. **Yu H, et al.** 2008. High-quality binary protein interaction map of the yeast interactome network. Science **322**:104–110.